Investigation of Aircraft Panel Deformations during Riveting Process

Abdelal, G. F., Georgiou, G., Cooper, J., Murphy, A., Robotham, A., & Lunt, P. (2014). *Investigation of Aircraft Panel Deformations during Riveting Process*. Paper presented at 4th Aircraft Structural Design Conference , Belfast, United Kingdom. http://www.aerosociety.com/Assets/Docs/Events/740/740_programme_print.pdf

Document Version:
Peer reviewed version

Investigation of Aircraft Panel Deformations during Riveting Process

Gasser F. Abdelal [1]
School of Mechanical and Aerospace Engineering, Queens's University, Belfast, UK, g.abdelal@qub.ac.uk, phone: +44 (0)28 9097 4123, Fax: +44 (0)28 9097 4148

Georgia Georgiou [2]
The Virtual Engineering Centre, University of Liverpool, Warrington, UK, G.Georgiou@liverpool.ac.uk

Jonathan Cooper [3]
Airbus Sir George White Chair, Faculty of Engineering, University of Bristol, Bristol, UK, j.e.cooper@bristol.ac.uk

Adrian Murphy [4]
School of Mechanical and Aerospace Engineering, Queens's University, Belfast, UK, a.murphy@qub.ac.uk

Antony Robotham [5]
Auckland University of Technology, New Zealand, tony.robotham@aut.ac.nz

Peter Lunt [6]
Airbus UK Ltd, Chester, UK, Peter.Lunt@Airbus.com

Abstract

In collaboration with Airbus-UK, the dimensional growth of small panels while being riveted with stiffeners is investigated. The stiffeners have been fastened to the panels with rivets and it has been observed that during this operation the panels expand in the longitudinal and transverse directions. It has been observed that the growth is variable and the challenge is to control the riveting process to minimize this variability. In this investigation, the assembly of the small panels and longitudinal stiffeners has been simulated using low and high fidelity nonlinear finite element models. The models have been validated against a limited set of experimental measurements; it was found that more accurate predictions of the riveting process are achieved using high fidelity explicit finite element models. Furthermore, through a series of numerical simulations and probabilistic analyses, the manufacturing process control parameters that influence panel growth have been identified. Alternative fastening approaches were examined and it was found that dimensional growth can be controlled by changing the design of the dies used for forming the rivets.

Introduction

Aircraft wings are typically composed of spars (longitudinal members) and ribs (transverse members) covered by skin panels. In this study, the focus has been on skin panels made of aluminium alloy and stiffened by longitudinal stringers, which are fastened to the skin panels with rivets. During the riveting cycle, clamps are applied to the skin-stringer assembly at pre-defined locations, a hole and countersink is drilled, the slug rivet inserted and formed, and the formed rivet head is milled flush with the panel surface. Each rivet is formed when head and the tail dies are forced together. The time to carry out the forming procedure can be as short as 3 milliseconds, during which time large plastic deformations of the slug rivet are experienced that create significant localised heating of the rivet material and high strain rates of around 10^3 sec^{-1}. The large diametrical expansion of the slug rivet creates a residual compressive stress field in the adjacent material around the hole, improving the fatigue life and the fluid retention of the joint. Usually, the rivet joint quality is affected by many parameters, such as plate thickness, rivet diameter, rivet pitch and squeeze force. Muller [14] showed that the squeeze force has the most significant role, and that a properly riveted joint using a high squeeze force can have three times the fatigue life of lower squeeze force rivets. The fastening process has been investigated experimentally and numerically by many researchers [1-5,15]. Their work was focused mainly on how the geometrical and manufacturing parameters of the process (squeeze force, rivet type and plate material) affect the induced residual stresses around the joint and the fatigue performance of a single rivet specimen. In large aircraft skin panels where several thousand rivets are inserted, it has been observed that the skin panels can undergo expansion in the longitudinal direction as a consequence of the fastening process. Experience shows that this panel growth is variable in nature so the challenge for manufacturing is to be able to control the production process to minimise growth. Numerical simulation methods have been used to investigate the skin panel growth due to the fastening process of multiple rivets. Low and high fidelity nonlinear finite element models of the single rivet forming were initially developed and validated against experimental data. These models were then used to predict the longitudinal deformation of small panel assemblies with multiple rivets. The simulation results were compared against experimental measurements obtained from a series of small panel samples that represented a range of different panel/stiffener thicknesses and rivet types. Alternative designs for rivet dies were examined for single and multiple rivet insertions; an alternative riveting process is proposed that reduces longitudinal growth of the panel. Finally, the manufacturing uncertainty during the riveting process was investigated on the small panel samples for different material configurations, different rivet pitch distances and variable loading conditions. The contribution of this study is tackling an area that has not been investigated before. This study is to focus on the riveting process parameters, such as head die design, impact force, rivets pitch and material type on the aircraft panel deformations. Some selected parameters are studied using high fidelity model, such as head die design and impact force, while other parameters are studied using low fidelity model. Studying the effect of the stochastic nature of selected parameters is very time consuming and requires low fidelity model to study it. This paper is the initial step to improve riveting manufacturing process of aircraft panels by exploring the parameters design space and recommending future research to follow.

Modelling and Simulation of Single Rivet Process

Low Fidelity Model

Low fidelity models are more practical to simulate the effect of hundreds of rivets on aircraft panels' assembly, as they are less expensive than high fidelity models. In addition, they are more efficient to use to study the stochastic nature of the riveting process as it will be shown later in the paper. A low fidelity model for predicting the induced residual stresses due to the riveting process was created and compared against the experimental measurements conducted by Withers [7] on a single rivet sample. The modelling scheme used was based on the work of Jachimowicz [12], where orthotropic thermal expansion of the rivet (axial-radial-tangential) was considered and temperature boundary conditions on the body of the rivet were applied in an effort to simulate the expansion and contraction of the rivet. The temperature boundary conditions were specified from the work of Repetto [8]. In this model, heat transfer between the rivet and the panel was not taken into account. The single rivet sample is of 5/16" diameter, while the panel and stiffener thicknesses were 15mm and 8.5mm, respectively [7]. The rivet dimensions are shown in Fig. 1-a. The centre part of the rivet is equivalent to the rivet hole dimensions, the tail part dimensions agrees to the standard 5/16" deformed rivet, while the head part is used to produce the squeeze effect along the rivet longitudinal axis. The finite element model of the single rivet specimen is shown in Fig. 1-b. Tetrahedral solid elements were used for the discretisation of the model, where the panel, stiffener and rivet were modelled as one part and different material type for each region was defined. The symmetry boundary conditions are applied to model only quarter of the model, while the far end plan is fixed in 3 directions.

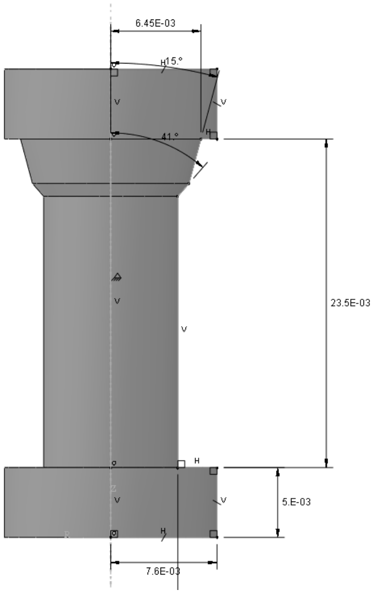

Fig. 1-a Deformed rivet dimensions.

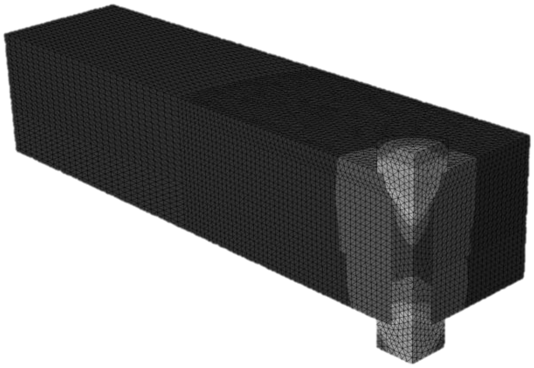

Fig. 1-b Von Mises stress distribution on the single rivet sample.

The main objective of the single rivet model was to predict the stress field due to the rivet insertion by varying the applied temperature boundary conditions and the material thermal expansion coefficients. Selecting the temperature to be 270^{0}C and the expansion coefficients (axial-radial-tangential) to be -0.0002, 0.0001, 0.0001 1/^{0}C, respectively, the developed residual tangential and radial stresses are shown in Fig. 2-a and Fig. 2-b. Direct comparison of the numerical results and experimental data presented by Fox and Withers [7] provided a level of confidence about this low-fidelity modelling approach, although there is some discrepancy between results closer to the rivet centre. Yet, the running time of the low fidelity model makes it very attractive for studying the stochastic nature of some selected parameters as discussed later in this paper. The current low fidelity model is capable to modelling residual stresses due to rivet insertion, but comes short to model the effect of head die design or the high-strain rate deformations near the rivet centre or the stress wave propagation due to impact load. This shortage led to studying the effect of these parameters using high fidelity model. It is recommended for future investigation to develop the low fidelity model to simulate more parameters, which leads to studying the stochastic nature of more parameters.

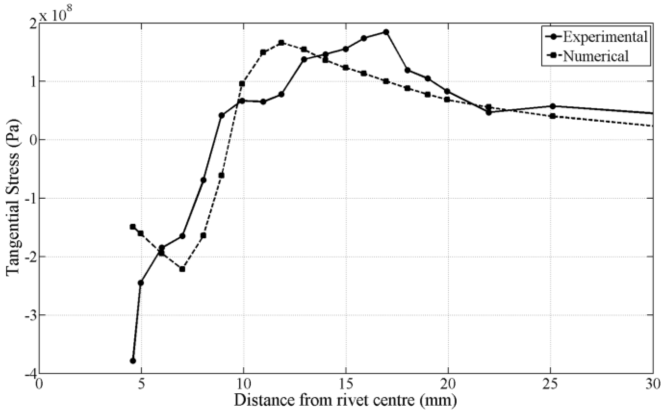

Fig. 2-a Numerical and experimental [7] residual tangential stresses along the countersink line.

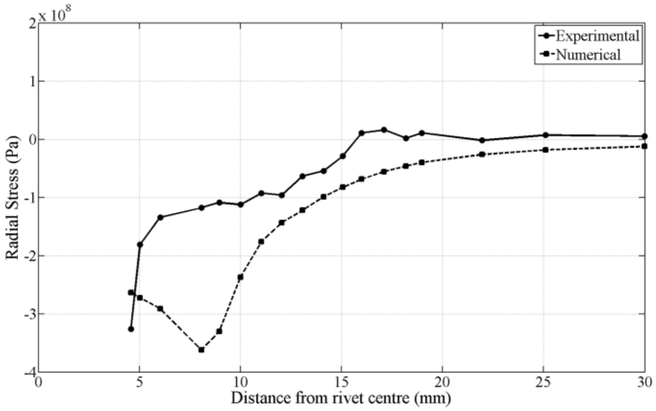

Fig. 2-b Numerical and experimental [7] residual radial stresses along the countersink line.

High Fidelity Model of the Single Rivet Insertion

In an attempt to achieve a more accurate correlation with the experimental results [7], a high-fidelity finite element model, which included nonlinear material properties, nonlinear boundary conditions (contacts) and large deformations, was created. This nonlinear finite element model is shown in Fig. 3 along with the areas that are clamped during the riveting process. The single rivet sample is of 5/16" diameter, while the panel and stiffener thicknesses were 15mm and 8.5mm, respectively. The maximum tolerance between rivet diameter and panel insertion hole is used (0.08 mm). Investigating the effect on geometrical tolerance on panel deformations is not the focus of this study.

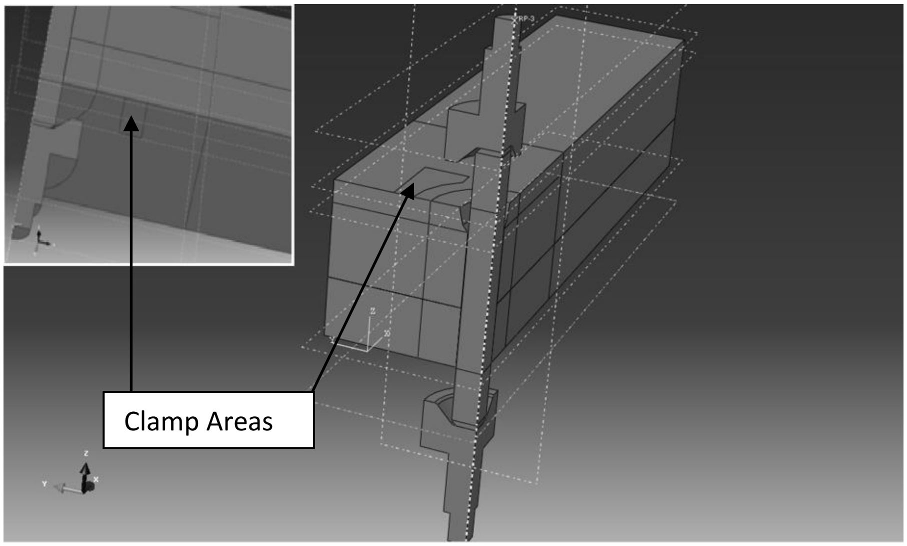

Fig. 3 Nonlinear finite element model for simulating single rivet insertion.

The clamping areas were constrained in x, y and z directions, assuming that the clamping and friction force fix the assembly. The applied squeeze force is incrementally increased and decreased following a triangular form over a time of 1ms, which reflects the duration of this process. The amplitude of the impact force applied on the head and tail die had a maximum value of 380kN and 400kN, respectively, at 0.5ms. Additionally, appropriate symmetry boundary conditions were considered and only a quarter of the small panel assembly was modelled. Furthermore, the geometrical form of the tail die and the head die were modelled as rigid bodies and general contacts were defined between all the assembly components (rivet - dies - panel - stiffener). The model was meshed with hexagonal elements, as they are more appropriate for material forming simulations. The rivet was meshed with elements of size (0.25 mm), while the panel and stiffener volumes near the rivet were meshed with elements of size (0.5 mm). In addition, a frictionless contact between the rivet and the panel was considered, as typically rivets are coated with an anodic coating. The friction coefficient between the dies and the rivet was assumed to be (0.47) [8], while the friction coefficient between the panel and the stiffener was selected to be (1.3) [8]. The material models used in this nonlinear finite element analysis reflected the impact of the high strain rate and the heat generated in the rivet on the resultant residual stresses and the displacement wave progress. The standard stress-strain curve was not appropriate for this type of analysis to model the rivet deformations, where high strain rates were encountered. Consequently, a Johnson-Cook plasticity model was used in order to describe the nonlinear behaviour of the rivet. The material type used for the rivet is an undisclosed AA2XXX alloy, similar in composition to AA2024-T3, while the material type used for the panel and stringer is undisclosed AA2XXX alloy, similar to AA2024-T351. More specifically, the Mises plasticity model with analytical forms of the hardening law and rate dependence, suitable for high-strain-rate deformation, was adopted. Johnson-Cook hardening is a particular type of isotropic hardening, where the static yield stress is assumed to be of the form

$$\bar{\sigma} = \left[A + B\left(\bar{\varepsilon}^{pl}\right)^{n} \right]\left[1 + C\ln\left(\frac{\dot{\bar{\varepsilon}}^{pl}}{\dot{\varepsilon}_0}\right)\right]\left(1 - \left(\frac{T}{T_{melt}}\right)^{m}\right), \tag{1}$$

where $\bar{\varepsilon}^{pl}$ is the equivalent plastic strain and A, B, C, $\dot{\varepsilon}_0$, n and m are material parameters measured at or below the transition temperature (T_{trans} = 25^0C). The Johnson-Cook material parameters are listed in Table 1.

Table 1 material mechanical property [9].

Material Type	***Aluminum 2017-T4***
Johnson-Cook parameters	A = 369 MPa - B = 684 MPa n = 0.73 - m = 1.7 C = 0.0083 - ε^o = 1 T_{melt} = 775 K

The applied squeeze force was set such that the rivet expansion at predefined locations matched manufacturing requirements. The amplitude of the squeeze force was selected to be 38kN on the head die, while the amplitude of the force was 40kN on the tail die. The predicted expansion of the rivet from the nonlinear finite element simulation, shown in Table 2, has excellent agreement with production requirements. The rivet expansion limits were of the order of 0.3mm, indicating that the squeeze force applied on the dies can be reduced, leading to lower longitudinal growth.

Table 2 Rivet expansion values.

	Rivet Expansion Finite Element Model
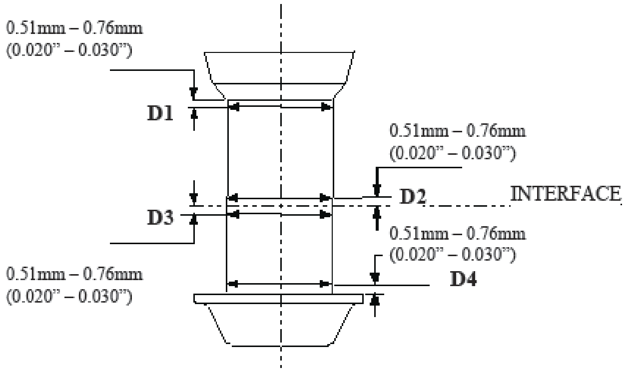	D1 = 0.560 mm D2 = 0.390 mm D3 = 0.386 mm D4 = 0.514 mm

Furthermore, the residual tangential and radial stresses (σ_{xx}, σ_{yy}) along the countersink line, that were predicted from the nonlinear finite element model, were compared against the experimental results of the physical prototype, as seen in Fig. 4-a and Fig. 4-b, respectively, demonstrating a high level of correlation compared to the lower fidelity model (Fig. 2-a and Fig. 2-b).

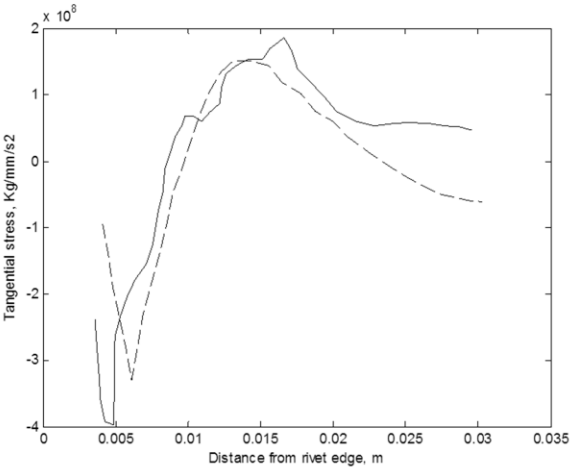

Fig. 4-a Numerical (dashed line) and experimental (solid line) [7] residual tangential stresses along the countersink line.

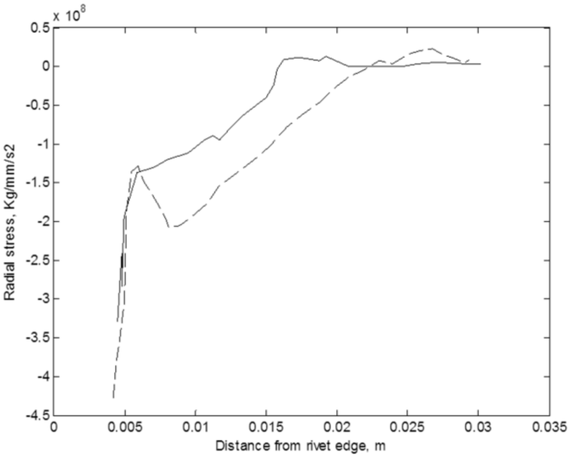

Fig. 4-b Numerical (dashed line) and experimental (solid line) [7] residual radial stresses along the countersink line.

Multiple Rivets Simulation with different Dies

A high-fidelity finite element model, which included nonlinear material properties, nonlinear boundary conditions (contacts) and large deformations, was created in an effort to study and simulate the panel growth on small panel assemblies due to the insertion of rivets. This nonlinear finite element model is shown in Fig. 15 along with the applied boundary conditions. The assembly was assumed to be compressed by aluminium plates with a spring mechanism on the left edge against the holding fixture, while on the right edge symmetry boundary condition was applied. An additional symmetry boundary condition was also applied at the XZ-plane of the coupon and as a result, only a quarter of the small panel assembly was modelled. The clamping force of the stand was replaced by an enforced compressing displacement and an appropriate coefficient of friction between the clamp and the assembly was applied. The finite element model resembled a small panel assembly from Category-4 (Table 3), with panel thickness 15.07 mm and stiffener thickness 9.0 mm. The element size, the material properties and the contact definitions were chosen to be similar to the single rivet finite element model described in Section 2.2.

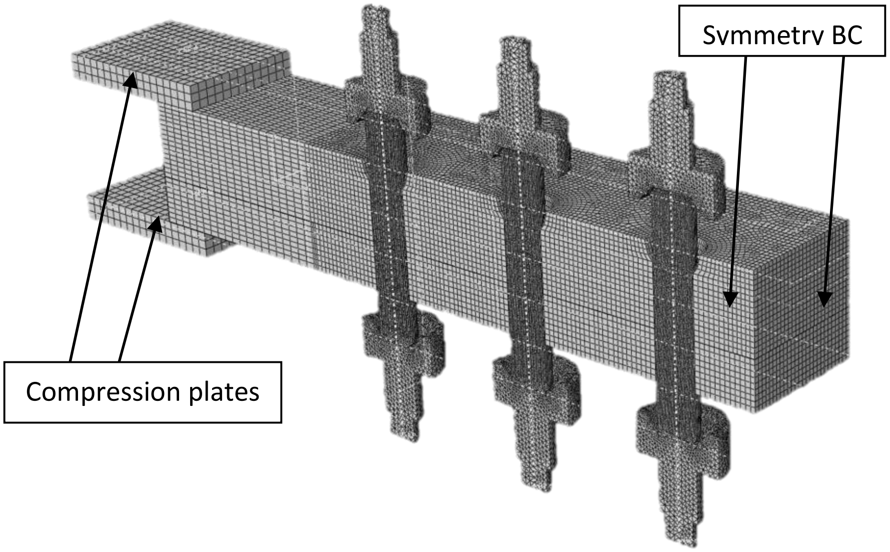

Fig. 15 Nonlinear finite element model for simulating the insertion of rivets on small panel assembly (Type 1).

During the simulation process, the boundary conditions of the assembly were adjusted in order to match the experimental results. In particular, the value of the compression displacement between the panel and the top clapping plate was selected to be 0.027mm. As a result, the predicted panel growth was 0.163mm (experimental 0.17mm) and the stiffener growth was 0.15mm (experimental 0.15mm). This step was performed to exclude the effect of boundary conditions in the finite element model, then other parameters will be varied and their impact on panel deformations is studied in the next section.
Furthermore, it is apparent, Fig. 16, that during the rivet head deformation under impact squeeze force from the head die, an excess volume of rivet material is gathering under the head die. As the rivet head material is plastically deformed under high strain rate, it would require a higher squeeze force to deform the rivet and satisfy the rivet expansion limits as described in Table 2 (due to the hardening of the material under compression). The higher squeeze force produces higher compression on the panel (higher residual stresses), which in turn leads to higher longitudinal growth. Comparing the possible rivet head material flow to the alternative head die design in Fig. 5, and the stress wave results discussed in the previous section, recommends the simulation of the experimental riveting using different head die design. Then compare the impact of each different head die on the panel deformations.

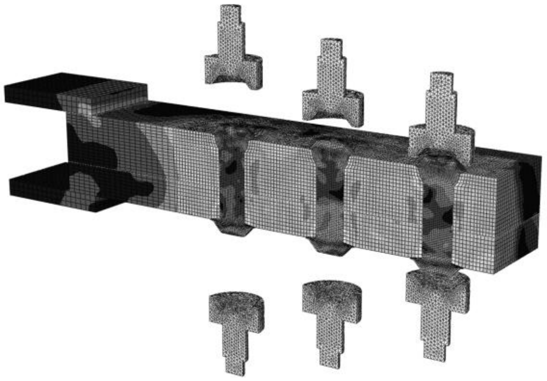

Fig. 16 Deformed small panel assembly after the rivet insertion process.

Alternative Die Designs

Alternative, an alternative head die design was examined for multiple rivet insertions while an alternative riveting process was also studied and compared against the original panel assembly and riveting process.

Multiple Rivet Insertions

The effect of alternative head die designs on longitudinal growth was further investigated through two discrete manufacturing processes, which included multiple rivet insertions on the small panel assemblies. In particular, the first scenario included the replacement of the original head die by an alternative design, while in the second scenario only the tail of the rivet was deformed. The first approach was simulated using the same rivet length and squeeze forces on dies, clamping loads on the panel and boundary conditions, as in the original assembly of the small panel assembly (Section 3.2). The design variant no.1 for the head die was proposed as a replacement candidate over the original geometry, the nonlinear finite element model of the coupon assembly is shown in Fig. 17. The selected die design requires lower squeeze force to deform the rivet, as the rivet material is free to deform in the transverse direction, and there is no excess material collected under the head die. Using the proposed design variant of the head die, a 6.1% reduction of the longitudinal growth was achieved. In an effort to avoid excessive deformation of the rivet head (Fig. 17), the squeeze force on the head die can be reduced by 13%, which leads to a 76.5% reduction in panel deformation, while satisfying the rivet expansion limits. An alternative riveting method, shown in Fig. 18, was also examined [13]. Similar considerations, regarding the clamping forces of the assembly and boundary conditions, as in the original assembly (Section 3.2), were made. During this process, only the tail of the rivet was deformed, while the head of the rivet was kept fixed. This formation requires the head of the rivet to be manufactured prior to the riveting process in the shape of the countersink hole on the panel. In Table 4, the rivet expansion values that were measured on the panel assembly for the alternative head die design and the alternative riveting processes are compared against the corresponding numerical results from the original assembly (Table 2). It can be seen that applying the nominal squeeze force on the tail die, a 54% reduction of the panel growth and 21% increase of the stiffener growth was observed.

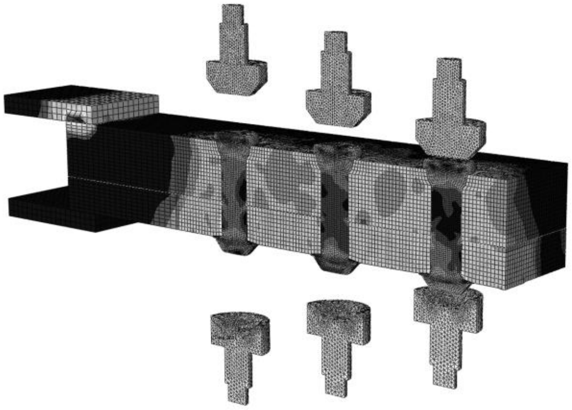

Fig. 17 Deformed panel assembly after the rivet insertion process for an alternative head die design.

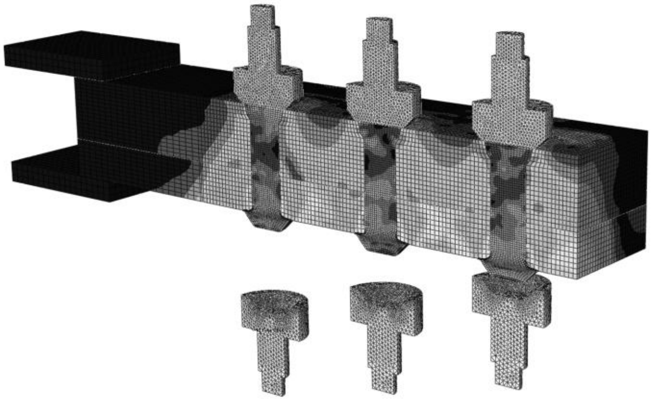

Fig. 18 An alternative riveting process with fixed head of the rivets.

The effect of alternative head die designs on longitudinal growth was further investigated through two discrete manufacturing processes, which included multiple rivet insertions on the small panel assemblies. In particular, the first scenario included the replacement of the original head die by an alternative design, while in the second scenario only the tail of the rivet was deformed. The first approach was simulated using the same rivet length and squeeze forces on dies, clamping loads on the panel and boundary conditions, as in the original assembly of the small panel assembly (Section 3.2). The design variant no.1 for the head die was proposed as a replacement candidate over the original geometry, the nonlinear finite element model of the coupon assembly is shown in Fig. 17. The selected die design requires lower squeeze force to deform the rivet, as the rivet material is free to deform in the transverse direction, and there is no excess material collected under the head die. Using the proposed design variant of the head die, a 6.1% reduction of the longitudinal growth was achieved. In an effort to avoid excessive deformation of the rivet head (Fig. 17), the squeeze force on the head die can be reduced by 13%, which leads to a 76.5% reduction in panel deformation, while satisfying the rivet expansion limits.

Table 4: Rivet expansion values for alternative head die design and riveting process.

Rivet Expansion Original head die	**Rivet Expansion Alternative head die**	**Rivet Expansion Alternative process**
D1 = 0.560 mm	D1 = 0.340 mm	D1 = 0.240 mm
D2 = 0.390 mm	D2 = 0.330 mm	D2 = 0.270 mm
D3 = 0.386 mm	D3 = 0.342 mm	D3 = 0.250 mm
D4 = 0.514 mm	D4 = 0.540 mm	D4 = 0.540 mm

These numbers reflect the huge impact of head die design on final panel deformations. Performing parameter sensitivity analysis of the head die dimensions with respect to panel deformation is recommended for future work as it is not practical to perform such analysis using the high fidelity model. If the low fidelity model is developed to simulate plasticity deformations and relate them to the head die design parameters, it would be more practical to perform design optimization of the head die dimensions and configurations. Low fidelity model is used in the next section to model stochastic process of selected riveting manufacturing process parameters, such as rivet pitch and assembly material type.

Uncertainty in the Manufacturing Process

Manufacturing uncertainty, related to variability in material properties, in applied boundary conditions from holding fixtures, in manufacturing loads as well as in environmental conditions, is not usually taken into account in tolerances specified in the manufacturing process. The stochastic nature of manufacturing processes is associated with significant increase in manpower requirements, manufacturing adjustments and delivery delays, affecting the product life cycle. In the current study, the impact of uncertainty in riveting process was investigated at the first level of the analysis test pyramid [10], which is widely used to categorise the testing in aircraft structures. The variability in panel growth due to the riveting process was examined in a deterministic and stochastic way using the small panel assemblies (Type 1) for different material configurations and different rivet pitch distances. The probabilistic analysis included multiple Monte-Carlo Simulations and the distribution of the panel growth due to varying loading conditions was predicted.

Model Description

The low-fidelity model of the single rivet insertion, described in Section 2.1, was implemented on the small panel assembly (Type 1) in an attempt to predict the panel growth. The examined panel was built with panel dimensions (279mm x 50 mm x 15 mm), the stiffener (279mm x 50mm x 8.5mm) and 6 rivets (3/8" diameter). Two discrete finite element models with different rivet pitch distances were generated, resembling the minimum allowable rivet pitch distance (38 mm) and the maximum rivet pitch distance (48 mm), respectively. The investigated finite element model of the small panel assembly for the case of the minimum rivet pitch distance is depicted at Fig. 19. Tetrahedral solid elements were used for the discretisation of the model, where the panel, stiffener and rivets were modelled as one part and different material type for each region were defined.

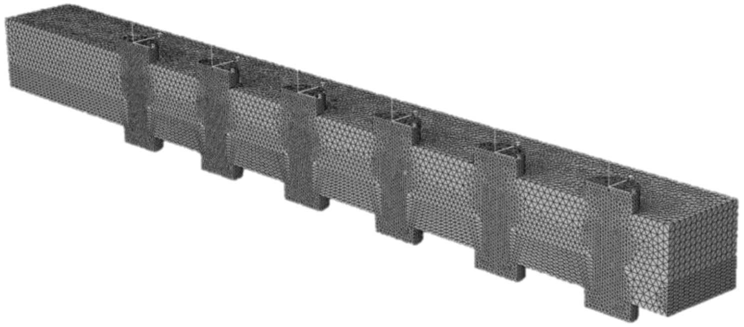

Fig. 19 Finite element model of the small panel assembly (Type 1) with minimum allowable rivet pitch distance.

The panel material was selected to be AA2024-T351 with Young's modulus 7.38E+10 N/m^2, Poisson's ratio 0.33 and density 2780 kg/m^3. The elastic-plastic hardening behaviour was taken into account according to the stain-stress curve (LT-Tension) included in Fig. A.1 [11]. Two cases for the material type of the stiffener were considered. Initially, the material of the stiffener was assumed to be Extruded AA2024-T3 with Young's modulus 7E+10 N/m^2, Poisson's ratio 0.33 and density 2780 kg/m^3, while the nonlinear behaviour of the material was described by the strain-stress curve (L-Tension) included in Fig. A.2 [15]. For the second case, the material type of the stiffener was selected to be AA2050-T84 with Young's modulus 7.6E+10 N/m^2, Poisson's ratio 0.33 and density 2780 kg/m^3, while the yield and the tensile strengths were considered as 4.75E+8 N/m^2 and 5.1E+8 N/m^2, respectively. Finally, the material for the rivets was selected to be AA2017-T4. The residual stresses around the rivets due to riveting process were generated by applying simultaneously the temperature boundary conditions at all rivets. The nonlinear finite element model was considered to be fixed at the right hand edge (Fig. 19), while the left hand edge of the assembly was constrained only along the z direction. Additionally, appropriate symmetry boundary conditions were applied and only the half of the model was simulated.

Deterministic Analysis

The low-fidelity approximation of the riveting process, described in Section 2.1, was applied on the small panel assemblies (Type 1) in an effort to predict the deformation for different rivet pitch distances and material configurations. Four deterministic nonlinear finite element analyses were conducted, considering the minimum and the maximum allowable rivet pitch distance as well as two discrete material types for the stiffener (AA2024-T3 and AA2050-T84), the calculated panel growth of the examined coupons is shown in Table 5.

Table 5: Panel growth of the process control coupons (Type 1).

Rivet Pitch Distance ***Stiffener Material***	***Minimum*** ***AA2024-T3***	***Maximum*** ***AA2024-T3***	***Minimum*** ***AA2050-T84***	***Maximum*** ***AA2050-T84***
Panel Growth (mm)	0.34	0.36	0.307	0.35

The numerical results in Table 5, show that the insertion of the rivets at the maximum pitch distance is leading to higher longitudinal growth, while the selection of the AA2050-T84 as the material type for the stiffener results in lower deformation. The higher longitudinal growth in the case of the maximum rivet pitch distance can be explained by inspecting Fig. 2-a and Fig. 2-b, and noticing that the residual stresses (tangential and radial) are decaying within a circle of 30 mm from the rivet center. As a result, in the case of two consquentive rivets, the stress fields developed around the rivets will share an overlapping region and will cancel each other (as stresses are acting in opposite directions) (Fig. 20).

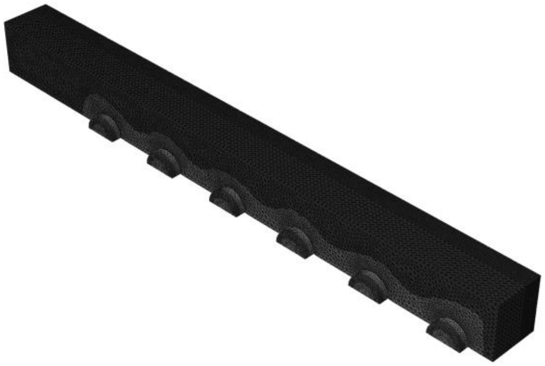

Fig. 20 Von Mises stress distribution on small experimental panel (Type 1) with minimum rivet pitch distance due to the riveting process.

Probabilistic Analysis

Different scenarios of probabilistic analyses were conducted in an effort to identify the influence of the applied temperature conditions on the panel growth, the small panel assembly (Type 1) was considered in two separate material configurations and two rivet pitch distances. The applied temperature conditions at each rivet for all the case studies were varied following a normal distribution with mean value 250^0C and standard deviation 10%. The averaged total elongation of the coupon was measured at the edge and on the centreline. At the first scenario, the material type of the panel and the stiffener was selected to be AA2024-T351 and AA2024-T3, respectively, while the minimum and maximum allowable rivet pitch distance was considered separately. 1000 Monte Carlo simulations were performed, changing independently each of the temperature conditions and the derived histograms of the probability density function are depicted at Fig. 21. The mean value of the averaged deformation was predicted to be 0.320mm and the standard deviation was 0.014mm for the minimum rivet pitch distance, while for the case of the maximum rivet pitch distance the averaged elongation was found to be 0.325mm and the standard deviation was 0.019mm. In the second scenario, the stiffener material was selected to be AA2050-T84 and considering the minimum or the maximum allowable rivet pitch distance, the derived histograms of the probability density function are depicted at Fig. 22. The mean value of the averaged growth was 0.280mm and the standard deviation was 0.013mm for the minimum rivet pitch distance, while for the case of the maximum rivet pitch distance the total deformation was predicted to be 0.318mm and the standard deviation was 0.019mm.

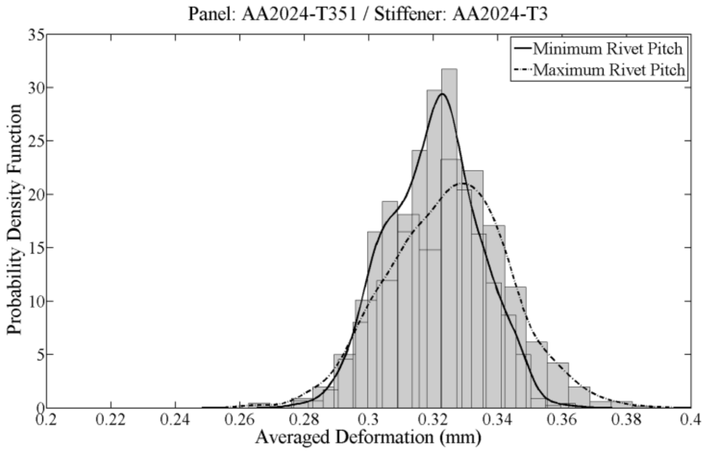

Fig. 21 Probability density function for small panel assembly (Type 1), AA2024 (T351-T3) material type and minimum/maximum rivet pitch distances.

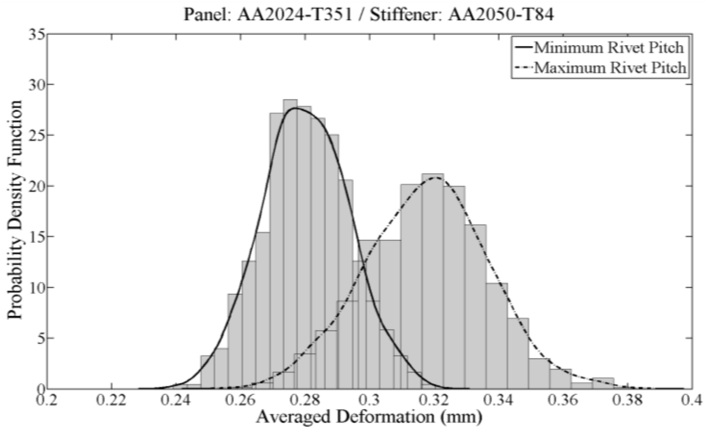

Fig. 22 Probability density function for small panel assembly (Type 1), AA2024-AA2050 material type and minimum/maximum rivet pitch

Inspecting Fig. 21 and Fig. 22, it becomes apparent that the selection of the material type for the stiffener significantly influences the growth of the small panel assemblies (Type 1), especially in the case of the minimum allowable rivet pitch distance. Additionally, the panels for both material configurations exhibited lower deformation for reduced rivet pitch distance due to the overlapping stress fields that were developed between the rivets and the cancellation of the residual stresses, as earlier. For the same reason, the probability density functions in the case of the minimum rivet pitch distance presented lower standard deviations leading to better predictability of the panel growth. Finally, the higher sensitivity of the small panel assemblies with material AA2024-AA2050 to the rivet pitch distance is due to the fact that the stiffener is stiffer than the panel leading to higher cancellation of the residual stresses for reduced rivet pitch distance in comparison to the panel with material AA2024 (T351/T3).

Conclusions

Alternative die designs and a different riveting process were investigated and proposed in an attempt to reduce the panel growth. Particularly, the deformations and the residual stresses around rivets developed due to riveting process using three alternative head die designs on single rivet samples were examined. Additionally, an alternative head die design and a different manufacturing method was studied separately on process control coupons (Type 1) predicting significant reduction on the panel growth, while satisfying the rivet expansion limits. Finally, a probabilistic analysis was conducted in an effort to quantify the uncertainty induced from the manufacturing process. From this analysis, it was found that the panel growth also depends upon the rivet pitch distance, the material of the stiffener as well as the manufacturing processing parameters (impact load, processing time).

Acknowledgments

This work is supported through the Virtual Engineering Centre (VEC), which is a University of Liverpool initiative in partnership with the Northwest Aerospace Alliance, the Science and Technology Facilities Council (Daresbury Laboratory), BAE Systems, Morson Projects and Airbus (UK). The VEC is funded by the Northwest Regional Development Agency (NWDA) and European Regional Development Fund (ERDF) to provide a focal point for virtual engineering research, education and skills development, best practice demonstration, and knowledge transfer to the aerospace sector.

References

[1] Deng, X., and Hutchinson, J.W., "The Clamping Stress in a Cold- Driven Rivet," *International Journal of Mechanical Sciences*, Vol. 40, No. 7, 1998, pp. 683–694.

[2] Langrand, B., Deletombe, E., Markiewicz, E., and Drazetic, P., "Riveted Joint Modeling for Numerical Analysis of Airframe Crashworthiness," *Finite Elements in Analysis and Design*, Vol. 38, No. 1, 2001, pp. 21–44.

[3] Li, G., and Shi, G., "Effect of the Riveting Process on the Residual Stress in Fuselage Lap Joints," *CASI Journal*, Vol. 50, No. 2, 2004, pp. 91–105.

[4] Ryan, L., and Monaghan, J., "Failure Mechanism of Riveted Joint in Fibre Metal Laminates," *Journal of Materials Processing Technology*, Vol. 103, No. 1, 2000, pp. 36–43.

[5] Szolwinski, M.P., and Farris, T.N., "Linking Riveting Process Parameters to the Fatigue Performance of Riveted Aircraft Structures," *Journal of Aircraft*, Vol. 37, No. 1, 2000, pp. 130–137.

[6] Rans, C., Straznicky, P.V., and Alderliesten, R., "Riveting Process Induced Residual Stresses Around Solid Rivets in Mechanical Joints," *Journal of Aircraft*, Vol. 44, No. 1, 2007, pp. 323-329.

[7] Fox, M.E., and Withers, P.J., "Residual Stresses in and Around Electromagnetically Installed Rivets Measured using Synchrotron and Neutron Diffraction, " *Journal of Neutron Research*, Vol. 15, No. 3-4, 2007, pp. 215-223.

[8] ASM Handbook, Volume 18 - Friction, Lubrication, and Wear Technology, 1992 ASM International.

[9] Gregory Kay, "Failure Modeling of Titanium 6A1-4V and Aluminum 2024-T3 with the Johnson-Cook Material Model, " Technical report Dot/FAA/AR-03/57, Lawrence Livermore National Laboratory, September 2003.

[10] Repetto, E.A., Radovitzky, R., Ortiz, M., Lundquist, R.C., and Sandstrom, D.R., "A Finite Element Study of Electromagnetic Riveting," *Journal of Manufacturing Science and Engineering*, Vol. 121, 1999, pp. 61-68.

[11] Deng, J.H., Yu, H.P., and Li, C.F., "Numerical and Experimental Investigation of Electromagnetic Riveting," *Materials Science and Engineering A*, Vol. 499, No. 1-2, 2009, pp. 242-247.

[12] Ostergaard, M.G., Ibbotson, A.R., Roux, O.L., and Prior, A.M., "Virtual Testing of Aircraft Structures," *CEAS Aeronautical Journal*, Vol. 1, No. 1-4, 2011, pp. 83-103.

[13] Niu, M.C.Y., *Airframe Structural Design*, Conmilit Press Ltd, Hong Kong, 1988.

[14] Kaniowski, J., and Jachimowicz, J., "Methods for FEM Analysis of Riveted Joints of Thin-Walled Aircraft Structures within the Imperja Project," *Proceedings of 25th ICAF Symposium*, Rotterdam, The Netherlands, May 2009.

[15] Hartmann, J., and Brown, T., "Integration and Qualification of the HH500 Hand Operated Electromagnetic Riveting System on the 747 Section 11," *Proceedings of the SAE Aerofast Conference & Exposition*, Wichita, KS, USA, September 1993.